Erratum

Expression of ceramide glucosyltransferases, which are essential for glycosphingolipid synthesis, is only required in a small subset of *C. elegans* cells

Esther Marza, Karina T. Simonsen, Nils J. Færgeman and Giovanni M. Lesa

Journal of Cell Science 122, 1700 (2009) doi:10.1242/jcs.052928

There was an error published in *J. Cell Sci.* **122**, 822-833.

The second sentence of the Introduction had a missing word, which altered the meaning. The corrected first paragraph is reproduced in full below.

Glycosphingolipids (GSLs) are complex glycolipids derived from ceramide. They consist of a ceramide lipid moiety (a fatty acid chain linked to a sphingoid base) embedded in the cell membrane, which is attached to a wide variety of oligosaccharide structures that extend from the non-cytosolic leaflet of the lipid bilayer (Degroote et al., 2004; Lahiri and Futerman, 2007). The ceramide is made in the endoplasmic reticulum (ER), and the oligosaccharide is synthesized in the Golgi complex by sequential addition of sugars to ceramide in the lumenal leaflet of the membrane. The precursor of most GSLs, glucosylceramide (GlcCer), is synthesized by ceramide glucosyltransferase (CGT) (Fig. 1), which catalyzes the addition of glucose to ceramide. More complex glycosphingolipids are generated by dedicated glycosyltransferases, which add further sugar molecules to GlcCer (Fig. 1) (Varki et al., 1999).

We apologise for this mistake.

Expression of ceramide glucosyltransferases, which are essential for glycosphingolipid synthesis, is only required in a small subset of *C. elegans* cells

Esther Marza[1], Karina T. Simonsen[2], Nils J. Færgeman[2] and Giovanni M. Lesa[1,3,*]

[1]MRC Laboratory for Molecular Cell Biology and [3]Department of Cell and Developmental Biology, University College London, Gower Street, London WC1E 6BT, UK
[2]University of Southern Denmark, Department of Biochemistry and Molecular Biology, Campusvej 55, 5230 Odense, Denmark
*Author for correspondence (e-mail: Giovanni.Lesa@ucl.ac.uk)

Accepted 26 November 2008
Journal of Cell Science 122, 822-833 Published by The Company of Biologists 2009
doi:10.1242/jcs.042754

Summary

Glycosphingolipids (GSLs) are glycosylated derivatives of ceramide in the lipid bilayer. Their ubiquitous distribution and complexity suggest that they have important functions, but what these are in vivo is still poorly understood. Here, we characterize the phenotype of *Caenorhabditis elegans* mutants with essentially no GSLs. The *C. elegans* genome encodes three ceramide glucosyltransferase (CGT) genes, which encode enzymes required for GSL biosynthesis. Animals lacking CGT do not synthesize GSLs, arrest growth at the first larval stage, and display defects in a subset of cells in their digestive tract; these defects impair larval feeding, resulting in a starvation-induced growth arrest. Restoring CGT function in these digestive tract cells – but not in a variety of other tissues – is sufficient to rescue the phenotypes associated with loss of CGT function. These unexpected findings suggest that GSLs are dispensable in most *C. elegans* cells, including those of the nervous system.

Supplementary material available online at
http://jcs.biologists.org/cgi/content/full/122/6/822/DC1

Key words: *C. elegans*, Ceramide, Glycosphingolipids, Glycosyltransferase, Intestine

Introduction

Glycosphingolipids (GSLs) are complex glycolipids derived from ceramide. They consist of a ceramide lipid moiety (a fatty acid chain linked to a sphingoid base) embedded in the cell membrane is attached to a wide variety of oligosaccharide structures that extend from the non-cytosolic leaflet of the lipid bilayer (Degroote et al., 2004; Lahiri and Futerman, 2007). The ceramide is made in the endoplasmic reticulum (ER), and the oligosaccharide is synthesized in the Golgi complex by sequential addition of sugars to ceramide in the lumenal leaflet of the membrane. The precursor of most GSLs, glucosylceramide (GlcCer), is synthesized by ceramide glucosyltransferase (CGT) (Fig. 1), which catalyzes the addition of glucose to ceramide. More complex glycosphingolipids are generated by dedicated glycosyltransferases, which add further sugar molecules to GlcCer (Fig. 1) (Varki et al., 1999).

GSLs are proposed to be important structural components of cell membranes and are particularly enriched in membrane microdomains known as lipid rafts. These domains are thought to help assemble signalling molecules and glycosylphosphatidyl-inositol-anchored proteins in specific membrane compartments, thus regulating signal transduction (Simons and Ikonen, 1997), although the existence and function of lipid rafts remains controversial (Munro, 2003).

Experiments in cell culture suggest that complex GSLs are involved in intracellular protein sorting (Sprong et al., 2001; Groux-Degroote et al., 2008), neuronal development (Futerman et al., 1999), cell growth and proliferation (Deng et al., 2000; Li et al., 2000), apoptosis (Kolesnick and Kronke, 1998), and cell adhesion and migration (Iwabuchi et al., 1998; Hakomori and Handa, 2002). However, analysis of mutant animals lacking enzymes important for GSL biosynthesis has failed to clarify the functions of GSLs in vivo. CGT-knockout mice, for example, which are unable to synthesize GSLs, die early during embryogenesis (E7.5-E9.5), with major defects in cell differentiation and a massive increase in apoptosis (Yamashita et al., 1999). It is not clear whether the increased apoptosis is caused by the accumulation of ceramide and its metabolites, which are known to promote apoptosis (Kolesnick and Kronke, 1998; Lahiri and Futerman, 2007), or by a lack of complex GSLs. However, apoptosis is apparently not increased in mice with CGT selectively knocked out in the nervous system, possibly because ceramide levels during development are not increased much in these animals, which display abnormal post-embryonic brain maturation (Jennemann et al., 2005). Surprisingly, several of the defects caused by CGT knockout in vivo are not observed in ES cells from CGT-deficient mice (Yamashita et al., 1999) or melanoma GM95 cells, which are devoid of GSLs (Ichikawa et al., 1994), suggesting that these lipids are particularly important for cell organization and differentiation in vivo. Knockout mice unable to synthesize a subset of complex GSLs, such as derivatives of gangliosides GM2, GD2 or GD3, display a variety of phenotypes, including disrupted male fertility, attenuated interleukin-mediated proliferative response of T cells, reduced regenerative capacity, motor deficits and neuronal degeneration caused by defects in myelination (Furukawa et al., 2004).

Because GSL-knockout studies in mammals have proved difficult to interpret, simpler model organisms have been used to investigate GSL function (Haltiwanger and Lowe, 2004). *Drosophila* CGT mutants are not available, but when CGT is

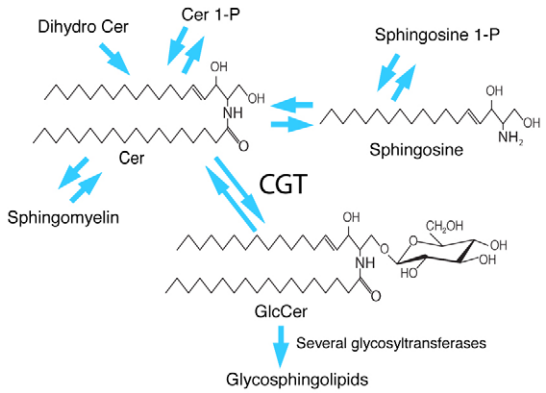

Fig. 1. Simplified GSL synthetic pathway. Glucosylceramide (GlcCer) is the precursor of all *C. elegans* glycosphingolipids. Cer, ceramide; CGT, ceramide glucosyl transferase.

knocked down by RNA interference (RNAi) in the fly embryo, apoptosis is increased (Kohyama-Koganeya et al., 2004). Moreover, deficiencies in the enzymes that add sugars to GlcCer lead to defects in several signalling pathways, including those activated by EGF receptors and Notch (Goode et al., 1992; Goode et al., 1996; Chen et al., 2007). Studies in *Caenorhabditis elegans* have also addressed important aspects of the physiological role of complex GSLs (GlcCer with additional sugars). Analysis of mutants resistant to the *Bacillus thuringiensis* toxin show that complex GSLs act in the intestine as toxin receptors and that the oligosaccharide chains are essential for this function (Griffitts et al., 2003; Griffitts et al., 2005). Additional studies show that mutations in genes involved in oligosaccharide addition to GSLs suppress gain-of-function mutations in *lin-12*/Notch, implying that complex GSLs act as positive regulators of Notch signalling (Katic et al., 2005). Recent work shows that mutations in genes required for the synthesis of C17 branched-chain fatty acids – which are normally incorporated into the GSL backbone – cause arrest at the first larval stage (L1) (Chitwood et al., 1995; Kniazeva et al., 2004; Entchev et al., 2008; Kniazeva et al., 2008). Mutant animals carrying these mutations have altered levels of C17 ceramides, as well as unusual ceramides (Entchev et al., 2008). It is possible that these alterations lead to reduced GSL function and L1 arrest. Interestingly, all the *C. elegans* mutants unable to synthesize complex GSLs are viable, suggesting that these lipids are dispensable in this organism, perhaps because the simple GSL GlcCer can functionally compensate for defects caused by complex GSL depletion or, alternatively, GSLs do not have essential functions. However, all these in vivo and in vitro studies have only partially clarified the physiological functions of simple GSLs, and it is still unclear whether all cells in *C. elegans* require these lipids, and, if so, for which physiological functions.

To answer these questions more definitively, we made *C. elegans* mutant strains that were unable to synthesize the GSL precursor GlcCer. In contrast to mammals and flies, which synthesize a single CGT protein, the *C. elegans* genome encodes three CGT proteins (Fig. 2), and we generated strains deficient in all of them. These mutants arrest at L1, become increasingly uncoordinated, and eventually die as L1 larvae. We characterize these mutants in detail and show that they are rescued by expressing CGT in a small number of cells in the intestinal tract, suggesting that CGT function is essential only in these cells.

Results

Generation of *cgt*-knockout animals

CGT transfers glucose from UDP-glucose to ceramide to form glucosylceramide, the precursor of all *C. elegans* GSLs (Fig. 1) (Ichikawa and Hirabayashi, 1998; Haltiwanger and Lowe, 2004). CGT is a transmembrane protein anchored to Golgi membranes through its N-terminus (Fig. 2A), with the active site facing the cytosol (Ichikawa et al., 1996; Marks et al., 1999). The amino acid sequence of CGT does not have immediately identifiable functional domains. However, site-directed mutagenesis associated with biochemical analysis in rat CGT showed that mutation of a conserved histidine (Fig. 2A, asterisk) in the UDP-glucose binding site of the protein causes a strong reduction of enzymatic activity. In addition, a detailed functional analysis has revealed that several conserved amino acids in the C-terminal two thirds of CGT (such as K124, D144, D236, R195, R272, R275, G224, G225 and W276) (Fig. 2A,B, green dots) are essential for enzymatic activity in vitro (Wu et al., 1999; Marks et al., 2001).

Blast analysis of the *C. elegans* genomic sequence revealed the presence of three genes highly homologous to the single mammalian *CGT* (*UGT8*) gene: *cgt-1*, *cgt-2* and *cgt-3* (Fig. 2A). The deduced protein sequences show a high level of identity with each other (at least 51%) and with mammalian CGT (37% identity for CGT-3 or CGT-2 and 34% for CGT-1) (Fig. 2C). Each amino acid essential for enzymatic activity is conserved in all three *C. elegans* CGTs, suggesting that they are functional proteins. Indeed, CGT-2 and CGT-3 have CGT activity when heterologously expressed in GM95 cells or in yeast cells (Ichikawa and Hirabayashi, 1998; Leipelt et al., 2001). To our knowledge, CGT-1 has not been tested for enzymatic activity. Based on the known expressed sequence tags and on serial analysis of gene expression tags, *cgt-3* is predicted to have four alternatively spliced mRNAs, all containing the amino acids essential for enzymatic activity (http://wormbase.org/db/gene/gene?name=WBGene00019127).

To investigate the role of GSLs in *C. elegans* and to determine the contribution of the three CGT genes, we used several CGT mutants. We generated the deletion *cgt-1(qa1809)* using PCR to screen chemically mutagenised *C. elegans* libraries with *cgt-1*-specific primers (Lesa, 2006). In addition, the deletion alleles *cgt-1(tm1027)*, *cgt-2(tm1097)*, *cgt-2(tm1192)* and *cgt-3(tm504)* were a generous gift from Shoehi Mitani (Tokyo Women's Medical University, Japan). All the *cgt-1* and *cgt-3* deletions (Fig. 2B) are likely to strongly reduce or completely eliminate CGT activity, because they lack several amino acids required for enzymatic activity (Marks et al., 2001). The *cgt-1*(*qa1809)* mutant lacks 908 bp that include exon 4 and exon 5 and part of exon 3 and exon 6, and therefore results in a protein with none of the required amino acids. The *cgt-1(tm1027)* mutant lacks 936 bp that include part of the *cgt-1* promoter, the start codon, the first three exons and part of exon 4, including K180 and D200. The *cgt-3(tm504)* mutant has a deletion of 1050 bp, which includes part of exon 2, the whole of exon 3 and exon 4, and the majority of exon 5, and inserts 57 new nucleotides, resulting in a protein that lacks the entire CGT gene active site. The *cgt-2(tm1097)* and *cgt-2(tm1192)* mutants contain a deletion of a small portion of exon 4 and part of the following intron (Fig. 2B). To test whether these deletions are likely to cause loss of CGT-2 protein function, we analyzed *cgt-2* mRNA transcripts by performing RT-PCR. Both *cgt-2(tm1097)* and *cgt-2(tm1192)* mutants produce a major and a minor mRNA transcript (Fig. 3). We sequenced the cDNAs derived from these transcripts and found that the protein corresponding to the major *tm1097* transcript is

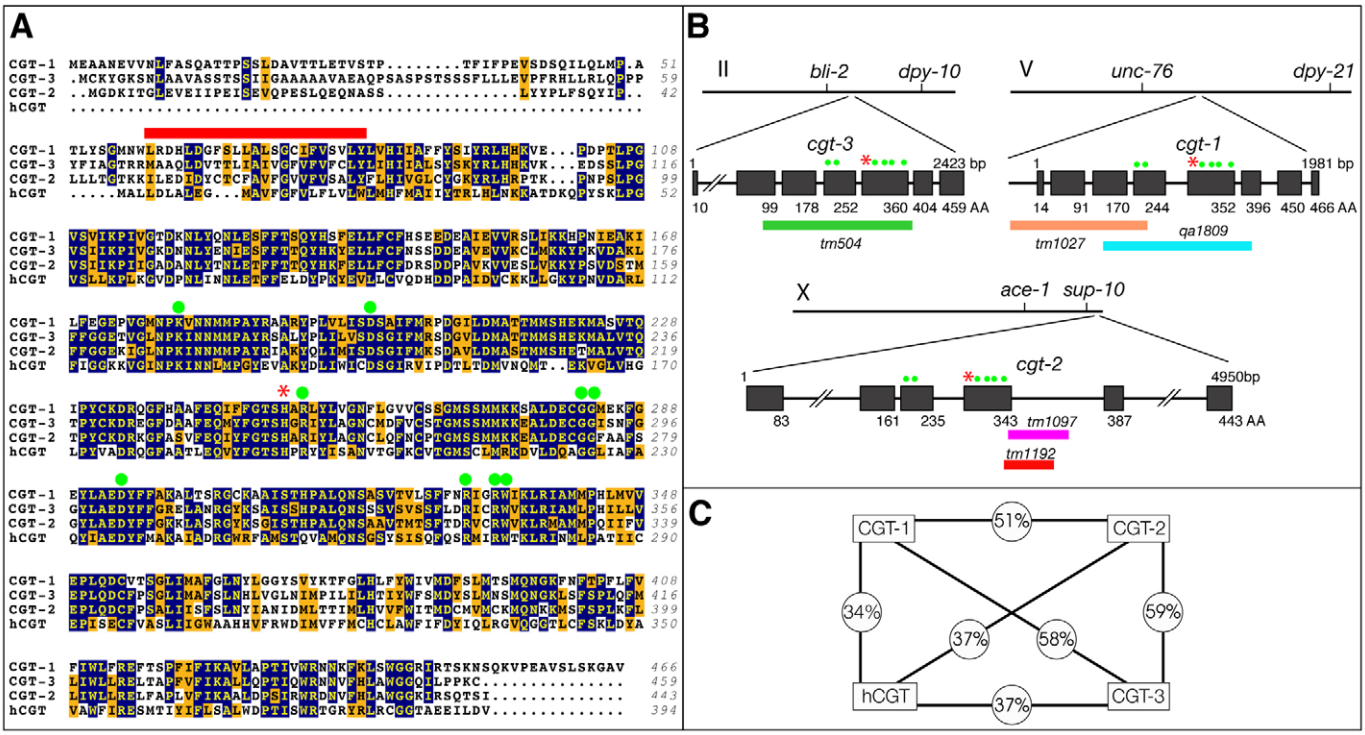

Fig. 2. *cgt-1*, *cgt-2* and *cgt-3* encode ceramide glucosyltransferases. (A) ClustalX alignment of CGT-1, CGT-2 and CGT-3 proteins with human CGT. Single-letter abbreviations for amino acid residues are used. Identical and similar amino acids are identified by dark blue and orange shading, respectively. The putative transmembrane domain is indicated with a red line. The asterisk indicates a conserved histidine in the UDP-glucose binding pocket essential for optimal enzymatic activity. Green dots indicate amino acids essential for enzymatic activity in vitro (Marks et al., 2001). (B) Genomic organization and deletions of the *cgt* genes. *cgt-3* is located on chromosome II, *cgt-1* on chromosome V and *cgt-2* on chromosome X. The coding regions are boxed and non-coding regions are shown as lines. Numbers at the top and bottom of each gene structure indicate nucleotide and amino acid sequences, respectively. The lines below each gene indicate deletions and their breakpoints. The asterisk and green dots are as in A. (C) Diagram of the comparison of identity among *C. elegans* and human CGT proteins. Percent identity at amino acid sequence level is shown.

truncated at W325, with the following seven new amino acids added: IASLLHS. Since *tm1097* does not remove amino acids known to be essential for CGT activity, it is not clear whether it causes loss of CGT-2 function. The protein corresponding to the major *tm1192* mRNA has a 31-amino acid deletion (313-343), which includes the required amino acids R321, R324 and W325 (Marks et al., 2001). It is therefore likely that *tm1192* results in complete loss of CGT-2 function. The minor *tm1097* and *tm1192* transcripts result in identical proteins lacking all amino acids encoded by exon 4 (Fig. 3) and are expected to produce mutant proteins with no enzymatic activity. All the *cgt* deletions we have used in this work, except *cgt-2(tm1097)*, are likely to completely eliminate CGT enzymatic activity.

Phenotype of CGT-knockout animals

All single CGT mutants showed no observable phenotype, suggesting that GSL levels might not be altered significantly in these mutants. Indeed, we found that levels of GlcCer derivatives in the putative null alleles *cgt-1(qa1809)* and *cgt-3(tm504)* were not affected in comparison with those of wild-type animals (Fig. 4, lanes 1, 2 and 7). Mutants carrying inactivated *cgt-2* in combination with inactivated *cgt-1* or *cgt-3* also did not display any observable phenotype. However, *cgt-3;cgt-1* double mutant animals arrested growth at an early larval stage and became increasingly uncoordinated and died after a few days (Fig. 5A,B). In addition, the growth-arrest phenotype caused by depletion of *cgt-1* and *cgt-3* activities by either gene deletion or by RNAi was not exacerbated by the presence of *cgt-2(tm1097)* or *cgt-2(tm1192)* or by RNAi for *cgt-2* (data not shown), suggesting that *cgt-2* does not influence the growth-arrest phenotype.

The *cgt-3;cgt-1* double mutants contained only ~25% of the GlcCer present in wild-type animals (Fig. 4, lane 6). Moreover, GlcCer levels were further reduced when all three *cgt* genes were knocked down (Fig. 4, lane 3), suggesting that *cgt-2* encodes a functional CGT protein. The level of GlcCer (7.5±1.3% of wild type) in the triple mutant might reflect an incomplete RNAi effect; it could represent GlcCer inherited from the mothers, which carry wild-type copies of *cgt-3* and have significant GSL levels, or it could represent maternal GlcCer, because some mothers could not be removed from the sample we analyzed. It is unlikely to reflect a dietary contribution, because, to our knowledge, *E. coli* (worm food) do not produce GlcCer.

Inspection under a dissecting microscope suggested that most *cgt-3;cgt-1* mutants arrested in L1 (Fig. 5A,B). Indeed, electron microscopy revealed that the arrested animals had alae, which are cuticular ridges only found in L1 larvae or adults (Fig. 5C). To determine how far development proceeded in L1, we focused on the M-cell lineage, which gives rise to sexually dimorphic muscles. L1 larvae hatch with one M cell (Fig. 5D), which divides after 5-6 hours at 20°C. The daughter cells then divide sequentially after ~3 hours, ~2 hours and ~3 hours, so that by the end of L1 (~15 hours after hatching) 16 M-lineage cells are present (Fig. 5E)

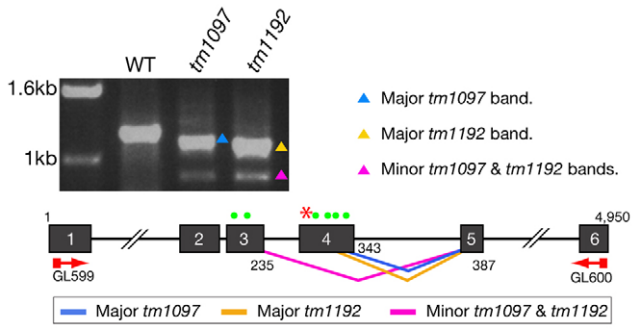

Fig. 3. Analysis of *cgt-2(tm1097)* and *cgt-2(tm1192)* mRNA. Gel showing the RT-PCR products of total mRNA extracted from wild-type, *cgt-2(tm1097)* or *cgt-2(tm1192)* animals with primers GL599 and GL600 (supplementary material Table S1). Both *tm1097* and *tm1192* mRNAs produce a major band and a minor band (triangles). Below is a schematic with the splicing products corresponding to the mutant bands. Boxes represent exons (numbered in white). Numbers at the top and at the bottom of *cgt-2* gene structure indicate nucleotide and amino acid sequence, respectively. The asterisk indicates the conserved histidine in the UDP-glucose binding pocket. Green dots indicate amino acids essential for CGT enzymatic activity (Marks et al., 2001).

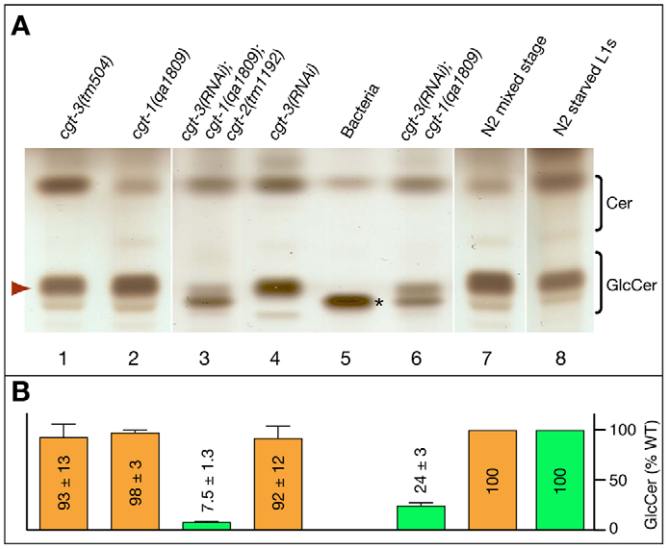

Fig. 4. Glucosylceramide levels in CGT mutant animals. (A) Thin-layer-chromatography analysis of polar lipids extracted from various CGT mutants (lanes 1-4 and 6) and from wild-type animals at different developmental stages (lanes 7 and 8). The origin is always at the bottom. The migration area of glucosylceramides (GlcCer) and ceramides (Cer) are indicated. A band similar to that observed in bacteria (asterisk) was present in other lanes. Since its intensity was proportional to the amount of bacteria in the sample, it is unlikely that wild-type animals produce lipids overlapping with this band. (B) Histogram showing the average relative intensity of the GlcCer bands, which include GSLs, from three separate experiments. GlcCer levels were not affected in *cgt* single mutants (lanes 1, 2 and 4), but were severely decreased when all CGT genes were knocked out or knocked down (lane 3). GSL levels from arrested CGT animals (lanes 3 and 6) were compared with those of starved wild-type L1 animals (lane 8). GSL levels from mixed-stage mutant populations (lanes 1, 2 and 4) were compared with those of mixed stage wild-type populations (lane 7). GlcCer levels in starved wild-type L1 animals were similar (89.8±6.1%; not shown) to those of wild-type animals (100%). The bands quantified (arrowhead in A) were those above the major bacterial band. Values are expressed as % wild-type ± s.e.m.

(Sulston and Horvitz, 1977). We used the integrated *hlh-8::gfp* reporter transgene to visualize the M cells, because it is specifically expressed in the M cell lineage (Harfe et al., 1998). Three days after hatching, more than 84% of the progeny of *cgt-3(RNAi);cgt-1* mutants had one or two GFP-positive cells, whereas all control animals had 16 GFP-positive cells (Fig. 5F), suggesting that most of the mutants arrested in early L1.

To verify that the growth-arrest phenotype is caused by inactivation of *cgt-1* and *cgt-3*, we performed transformation rescue experiments in animals with inactivated *cgt-1* and *cgt-3*. As shown in Table 1, expression of extrachromosomal copies of either *cgt-1* or *cgt-3* bypassed the growth arrest at L1 (Table 1). Moreover, a PCR fragment containing the promoter, coding region and 3′-untranslated regions of wild-type *cgt-1*, rescued the *cgt-3(RNAi);cgt-1(qa1809)* mutants as did wild-type *cgt-3* in *cgt-3(tm504);cgt-1(RNAi)* animals. These results show that the growth-arrest phenotype is caused by simultaneous inactivation of *cgt-1* and *cgt-3*.

CGT genes are required embryonically or during the first larval stage

To test when genes encoding CGTs are normally required to allow proper growth, we inactivated them at different developmental stages. First, we used *cgt-3* siRNA in *cgt-1* mutant mothers (n=12) and found that the progeny arrested at the L1 stage. However, when we exposed *cgt-1* mutant animals to *cgt-3* siRNA immediately after hatching (n=32), all the animals reached adulthood. These results suggest that *cgt-1* activity is either required embryonically or during the L1 stage, since *cgt-3* RNAi takes approximately 12-14 hours to produce the growth-arrest phenotype in *cgt-1(qa1809)* mutant animals at 20°C (G.M.L., unpublished results), which is roughly the duration of the L1 stage (Byerly et al., 1976). It is unlikely that CGT genes are required for general embryonic development, because, upon hatching, the *cgt-3;cgt-1* L1 larvae did not show gross morphological defects and we could rescue the *cgt-3;cgt-1* phenotype by tissue-specific expression of either *cgt-1* or *cgt-3* (see below). It is also unlikely that the L1 arrest is a maternal effect phenotype, because we observed an identical L1 arrest in progeny of *cgt-3;cgt-1(RNAi);cgt-2* mothers [RNAi often reduces stores of maternal message that would normally be inherited by the oocyte (Maine, 2001)] and in *cgt-3;cgt-1;cgt-2* progeny of *cgt-3;cgt-1/+;cgt-2* mothers (data not shown).

Apoptosis is unlikely to be the cause of the growth arrest

Apoptosis is dramatically increased in mice and *Drosophila* when CGT is knocked out, possibly because loss of CGT function causes accumulation of ceramide (Yamashita et al., 1999; Kohyama-Koganeya et al., 2004), a known inducer of apoptosis (Pettus et al., 2002). Since our lipid analysis revealed a modest increase in ceramide levels in mutants undergoing growth arrest (Fig. 4), we tested whether apoptosis has a role in the growth-arrest phenotype caused by simultaneous inactivation of *cgt-1* and *cgt-3*. In mammalian cells, overexpression of *BCL2*, an anti-apoptotic gene, suppresses ceramide-induced apoptosis (Zhang et al., 1996). Likewise, gain-of-function mutations of the *C. elegans* homolog *ced-9*, and loss-of-function mutations of two pro-apoptotic genes, *ced-3* (a caspase) and *ced-4* (the caspase activator apaf-1), suppress the death of all the cells that normally undergo apoptosis (Hengartner and Horvitz, 1994). Thus, if the growth arrest of *cgt-3;cgt-1* mutant animals is caused by excessive apoptosis, mutants carrying any of the CED protein mutations should grow normally.

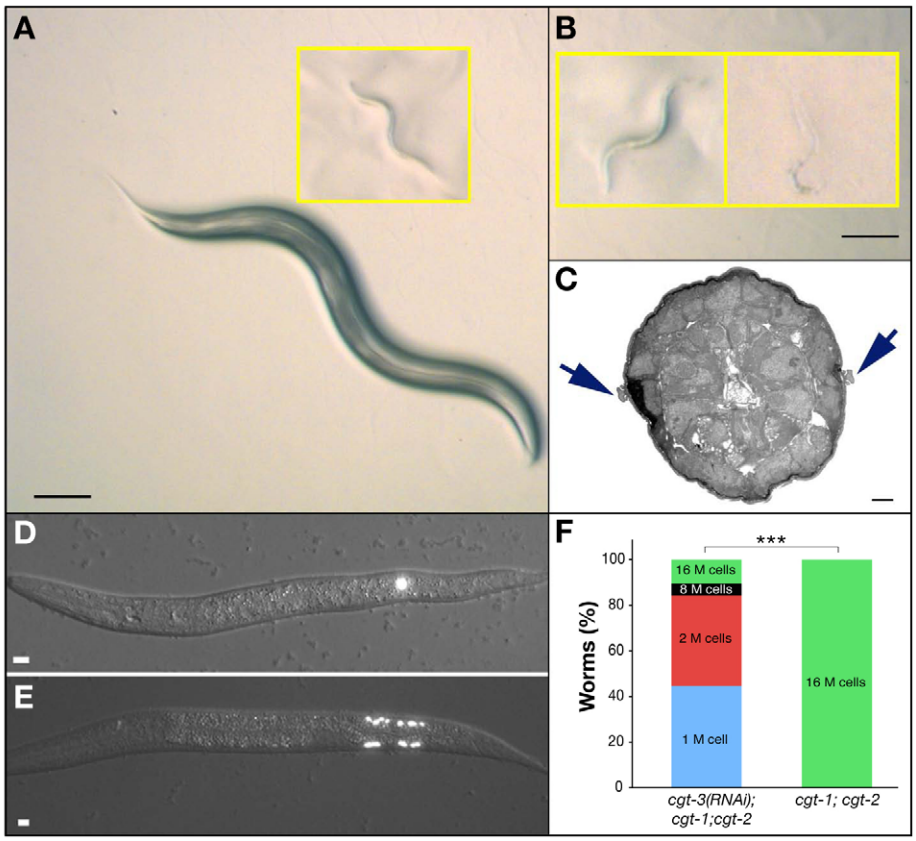

Fig. 5. Essentially eliminating CGT function results in arrest at the first larval stage (L1). (A) Wild-type animals or single CGT mutants reach adulthood within ~3.5 days at 20°C. The inset shows a wild-type L1 animal. Scale bar: 100 µm. (B) *cgt-3(RNAi);cgt-1(qa1809)* mutants appear normal as soon as they hatch (left inset), do not develop beyond the L1 stage and die after a few days (right inset). Scale bar: 100 µm. (C) Electron micrograph of a transverse section of an arrested *cgt-3(RNAi);cgt-1(qa1809)* mutant worm. Arrows indicate cuticular ridges (alae) present at the L1 stage but not at other larval stages. The *cgt-3;cgt-1* double mutant worm shown has therefore arrested at the L1 stage. Scale bar: 1 µm. (D,E,F) Worms carrying an integrated *hlh-8::gfp* reporter gene, which directs GFP expression in the M-cell lineage. M-cell number reflects the developmental stage of L1 larvae. Worms hatch with one M cell (D); subsequent divisions produce 2, 4, 8 and, by the end of L1, 16 M cells (E). Scale bars: 10 µm Approximately 45% of *cgt-3(RNAi);cgt-1(qa1809);cgt-2(tm1192)* worms arrested at the one-M-cell stage, 39% at the two-M-cell stage, 5% at the eight-M-cell stage and 11% at the 16-M-cell stage (F). ***P<0.0001.

To test this, we inactivated *cgt-1* and *cgt-3* by RNAi in *ced-3(n717)* (n=7), *ced-4(n1162)* (n=4) or *ced-9(n1950)* (n=6) mutant worms. All of the 17 animals exposed to RNAi produced progeny that arrested at the L1 larval stage, as did wild-type animals exposed to the same siRNAs (n=5). Moreover, we used the nucleic acid fluorescent dyes SYTO11 and acridine orange to visualize apoptotic nuclei. The nuclear staining pattern was similar in *cgt-3(RNAi);cgt-1(qa1809);cgt-2(tm1192)* arrested mutants and in wild-type animals (data not shown), suggesting that no additional apoptotic events were occurring in the mutants. In agreement with these results, we could not detect an increase in button-like cells (a typical apoptotic phenotype) under Nomarski optics in arrested mutants. It is therefore unlikely that the growth-arrest phenotype observed in *cgt-3;cgt-1* worms is caused by increased apoptosis.

CGT-1 and CGT-3 are expressed in several tissues but not in the nervous system

To gain insight into the function(s) of *cgt-1* and *cgt-3* we looked at where *cgt-1* and *cgt-3* are normally expressed. We generated constructs of *cgt-1* and *cgt-3* containing the endogenous promoter, the coding sequence fused in-frame with GFP, and the 3′ untranslated region. These constructs encode fully functional proteins, because they rescued the growth-arrest phenotype of *cgt-3;cgt-1* mutant animals. Their expression pattern is therefore likely to reflect that of the corresponding endogenous genes.

Both *cgt-1::gfp* and *cgt-3::gfp* were strongly expressed in pharyngeal muscles and in other pharyngeal cells, although their expression did not completely overlap (Fig. 6). In addition, they showed strong expression in the pharyngeal intestinal valve (PIV),

Table 1. Transformation rescue experiments in animals with inactivated *cgt-1*, *cgt-2* and *cgt-3*

Construct	Expressed in	Genetic background	Growth arrest rescue (lines)	
cgt-1p::cgt-1	Endogenous promoter	1, 2, 3	+	(5/5 lines)
cgt-3p::cgt-3	Endogenous promoter	2, 4	+	(2/2 lines)
myo-2p::cgt-1	Pharynx	1	–	(0/2 lines)
unc-119p::cgt-1	Neurons	5	–	(0/2 lines)
unc-119p::cgt-3	Neurons	5	–	(0/2 lines)
myo-3p::cgt-3	Most muscles	5	–	(0/2 lines)
unc-119p::cgt-3, myo-3p::cgt-3	Neurons and most muscles	5	–	(0/2 lines)
pF54D5.1p::cgt-1	PIV, IRV, intestine*	2, 6, 7	+	(6/6 lines)
pF54D5.1p::cgt-3	PIV, IRV, intestine*	2	+	(2/2 lines)
elt-2p::cgt-1 (2.5 ng/µl)	Intestine	1	+/–	(2/7 lines)
elt-2p::cgt-1 (10 ng/µl)	Intestine	1	+	(3/3 lines)

Genetic background of the strains used for rescue experiments: 1, *cgt-1(qa1809);cgt-3(RNAi)*; 2, *cgt-3(tm504);cgt-1(tm1027);cgt-2(RNAi)*; 3, *cgt-3(tm504);cgt-1(qa1809);cgt-2(tm1097);* 4, *cgt-3(tm504);cgt-1(RNAi)*; 5, *cgt-3(tm504);cgt-1(tm1027)*; 6, *cgt-3(tm504);cgt-1(tm1027);cgt-2(tm1192)*; **7**, *cgt-3(tm504);cgt-1(qa1809);cgt-2(tm1192)*. *Anterior and posterior intestine.

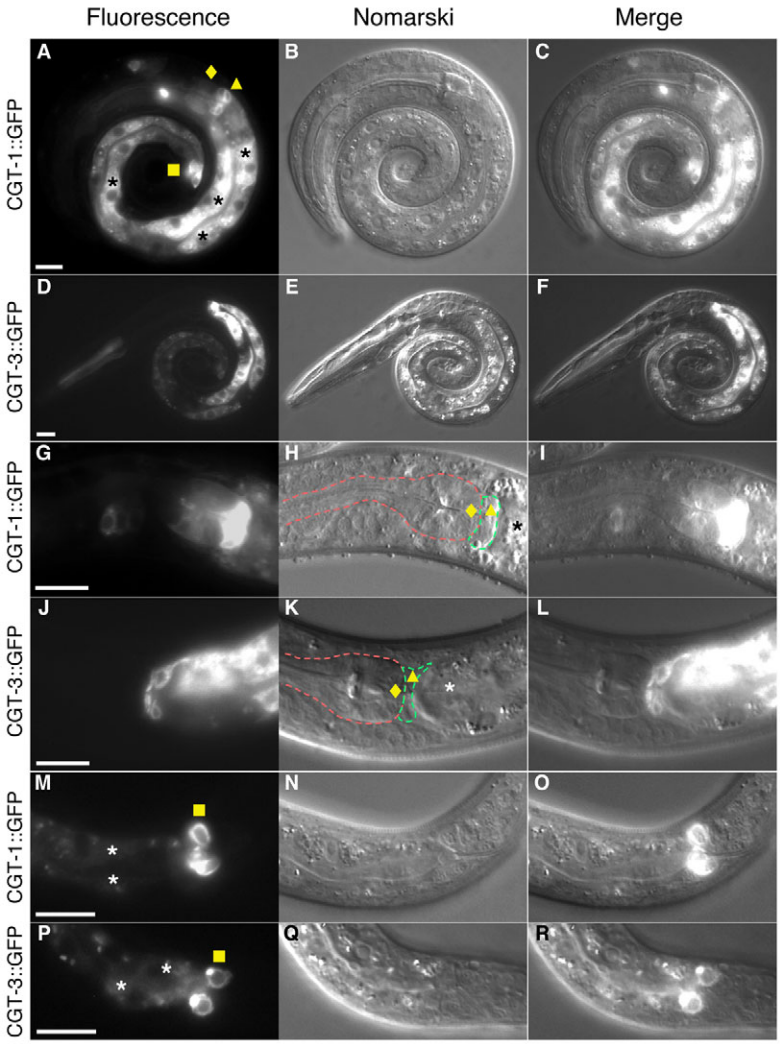

Fig. 6. Expression pattern of *cgt-1* and *cgt-3* in L1 larvae. CGT-1::GFP (A-C,G-I,M-O) and CGT-3::GFP (D-F,J-L,P-R) show both a strong signal in pharyngeal muscles (diamond), PIV (triangle), intestinal cells (asterisk), and IRV and RGCs (both indicated by a square). Close views of the PIV (G-L) and the IRV and RGCs (M-R) are shown. The pharynx is marked with a red dashed line; the PIV with a green dashed line. For expression in adults, see supplementary material Fig. S1. Scale bar: 10 µm.

a set of six epithelial cells connecting the posterior bulb of the pharynx to the anterior intestine (Hall and Altun, 2008), in the intestinal cells (particularly the most anterior and the most posterior), in the intestinal rectal valve (IRV), two epithelial cells that occlude the lumen of the posterior intestine, and in the three rectal gland cells (RGCs) (Hall and Altun, 2008). We detected *cgt-1::gfp* expression in the excretory cell, excretory canals, duct cell and pore cell; these cells form the excretory system, which helps to maintain osmotic or ionic balance and secretes material of unknown nature and function (Hall and Altun, 2008). Some *cgt-3::gfp* expression was also visible in head mesodermal cells. Both *cgt-1* and *cgt-3* showed additional, non-overlapping, expression in some non-identified head cells. Interestingly, with the possible exception of a few amphid neurons, we could not detect any expression of *cgt-1* or *cgt-3* in the nervous system.

CGTs are essential in a limited number of cells

To determine where the genes encoding CGT are essential, we tested whether a single wild-type copy of *cgt-1* is sufficient to rescue the growth-arrest phenotype in worms with no active genes encoding CGT. We produced the strain *cgt-3(tm504);cgt-1(qa1809)/DnT1;cgt-2(tm1192)*. *DnT1* is a reciprocal translocation between chromosomes IV and V, which contains wild-type *cgt-1*; therefore, the strain we produced contains *cgt-1* as the only *cgt* gene. We found that this strain did not arrest growth, indicating that the essential CGT function resides within the tissues where *cgt-1* is normally expressed (Fig. 6). Since we observed the growth-arrest phenotype only when both *cgt-1* and *cgt-3* were inactivated, it is likely that the essential CGT gene function is exerted in a tissue where both genes are normally expressed, that is the PIV, the IRV, the intestine, the RGCs and the pharyngeal cells. We therefore generated constructs that drive gene expression in specific tissues and tested their ability to rescue the growth arrest phenotype associated with loss of CGT activity. As expected, constructs containing the endogenous promoter, the coding sequence and the 3′ untranslated region of *cgt-1* or *cgt-3* restored normal growth of *cgt-3;cgt-1* or *cgt-3;cgt-1;cgt-2* mutant animals (Table 1).

To test whether GSLs can rescue the defect cell non-autonomously, we expressed CGT genes in muscles and in the nervous system, where no CGT expression is normally detected, and examined whether the growth-arrest phenotype of *cgt-3;cgt-1* mutant animals was rescued. We placed *cgt-3* under the control of the *myo-3* promoter, which drives expression in most muscles, and *cgt-1* and *cgt-3* under the control of the neuron-specific *unc-119* promoter. As expected, these chimeric constructs could not rescue

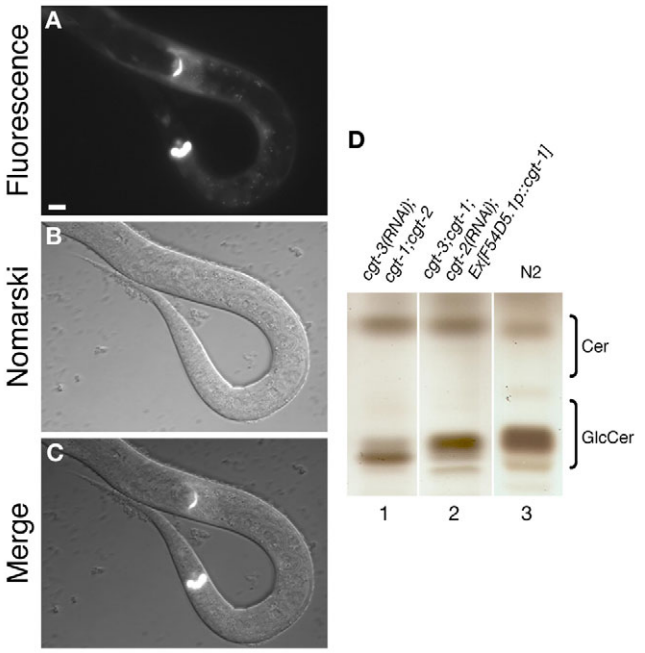

Fig. 7. GSL levels are close to normal in CGT triple mutants expressing *cgt-1* under the control of the F54D5.1 promoter. (A-C) *F54D5.1p::gfp* is expressed in a limited number of cells: the PIV, the IRV, the RGCs and often the most anterior and posterior intestinal cells. Scale bar: 10 μm. (D) Thin-layer-chromatography analysis of polar lipids extracted from CGT triple mutants (lane 1), triple mutants expressing *F54D5.1p::cgt-1* (lane 2) and wild-type animals (lane 3). Alleles: *cgt-1(qa1809)* (lane 1), *cgt-1(tm1027)* (lane 2), *cgt-2(tm1192)*, *cgt-3(tm504)*.

the growth-arrest phenotype of *cgt-3;cgt-1* double mutant animals, even when coexpressed (Table 1), suggesting that GSLs or their products do not effectively cross cell boundaries.

We then investigated whether a construct selectively driving *cgt-1* expression in the pharyngeal muscles (*myo-2p::cgt-1*) (Okkema et al., 1993) could rescue the growth arrest of *cgt-3;cgt-1* mutant animals. We generated several stable lines and found that this chimeric construct could not rescue growth arrest (Table 1), suggesting that CGT function is required in non-pharyngeal tissues to overcome the growth-arrest phenotype of *cgt-3;cgt-1* mutant animals.

We then tested whether *cgt-1* or *cgt-3* expressed in the PIV, IRV and a subset of intestinal cells could rescue the growth arrest of *cgt-3;cgt-1* or *cgt-3;cgt-1;cgt-2* mutant animals. We placed *cgt-1* and *cgt-3* under the control of the *F54D5.1* promoter, which drives expression specifically in PIV, IRV, the RGCs, and the most anterior and posterior intestinal cells from late embryonic stages until adulthood (Hope et al., 2004) (Fig. 7A-C and data not shown). Transgenic *cgt-3;cgt-1* double mutants, and even triple mutants expressing these constructs, grew and reproduced similarly to wild-type animals. In addition, they produced levels of GSLs close to (~70%) those of wild-type animals (Fig. 7D). These findings suggest that CGT function is required in the IRV, PIV, RGCs, a subset of intestinal cells, or in a combination of these cells.

To test whether intestine-specific expression of CGT was sufficient to rescue the *cgt-3;cgt-1* mutant phenotype, we placed *cgt-1* under the control of the intestine-specific promoter *elt-2* (Fukushige et al., 1998), which is expressed in the intestine and its precursor cells from early embryonic stages. This construct rescued the phenotype of *cgt-3;cgt-1* mutants. Since we also rescued the mutant phenotype by expressing CGT in PIV, IRV and in the most anterior and posterior intestinal cells, it is likely that CGT function is only required in the most anterior and posterior intestinal cells.

Why do CGT mutants arrest growth?

When *C. elegans* larvae hatch, they are developmentally arrested and require food to start and maintain normal post-embryonic development (Johnson et al., 1984; Hong et al., 1998). We therefore tested the possibility that *cgt-3;cgt-1* mutants arrest growth because they are unable to feed normally. We mixed small fluorescent beads (with a diameter of ~20% of that of the bacteria that the worms feed) with food and examined whether the beads appeared in the digestive tract of 1-day old, L1-arrested CGT mutants (Fig. 8). The vast majority of control *cgt-1;cgt-2* L1 larvae (85.1±3.3%) had multiple fluorescent beads along their digestive tract, and very few had no beads at all in the digestive tract (9.6±4.0%) or beads that had not passed the pharynx (5.3±1.8%) (Fig. 8A-C). By contrast, most of the L1-arrested *cgt-3(RNAi);cgt-1;cgt-2* mutants either had no fluorescent beads at all in their digestive tract (42.7±6.6%, $P<0.0001$) or had beads stuck (29.7±4.9%, $P<0.0001$) just before (Fig. 8D-F) or just after (Fig. 8G-I) the PIV. Only 27.6±5.4% ($P<0.0001$) of the mutants had beads inside the intestine. To confirm that CGT mutants were starved, we examined DAF-16::GFP (Fig. 8K-N), which is normally localized in the cytoplasm (Fig. 8K-M) but displays mainly nuclear localization under starvation and other stresses. DAF-16::GFP was mainly localized in the nucleus of arrested mutants (Fig. 8N), consistent with the animals being starved.

To test whether the PIV or the most anterior intestinal cells are defective in CGT mutants (beads tend to accumulate around the PIV) we used Nomarski and fluorescence microscopy and *F54D5.1::gfp* to visualize PIV and IRV. As shown in Fig. 9, these cells appeared normal in newly hatched *cgt-3(RNAi);cgt-1;cgt-2* mutants, and remained so 1 day after hatching, when the mutants already show defects in feeding. To check whether the canal formed by the PIV and the IRV cells was also normal in 1-day-old *cgt-3(RNAi);cgt-1;cgt-2* mutants, we used confocal microscopy in animals expressing *F54D5.1::gfp*, and performed three-dimensional reconstructions (supplementary material Fig. S2, Movies 1-3). The canal formed by the PIV cells had a similar area in control (not-arrested) L1 *cgt-1;cgt-2* larvae (3.27±1.06 μm^2, n=3) and in L1-arrested *cgt-3(RNAi);cgt-1;cgt-2* larvae (3.62±0.57 μm^2, n=10), suggesting that the feeding defect is not caused by a physical obstruction within the PIV. Similarly, no difference was detectable in the IRV canal (*cgt-1;cgt-2* mutant: 2.02±0.45 μm^2, n=3; *cgt-3(RNAi);cgt-1;cgt-2* mutant: 1.89±0.46 μm^2, n=15). However, after the first day of L1 arrest, most of the anterior intestinal cells appeared swollen and vacuolated: an appearance consistent with necrotic cell death. In addition, the intestinal tract appeared obstructed, and in some cases the lumen seemed discontinuous. Later, the PIV and IRV also became swollen (Fig. 9). The swollen and vacuolated cells displayed dispersed, faint or no *F54D5.1::gfp* expression in CGT mutants, which suggests that they are necrotic, whereas they looked normal and were normally fluorescent in starved control L1 larvae (Fig. 9), suggesting that the changes were not caused by starvation. Since the PIV and IRV cells became swollen after the intestinal cells appeared to degenerate, it is possible that the PIV and IRV abnormalities were secondary to the necrosis of the intestinal cells.

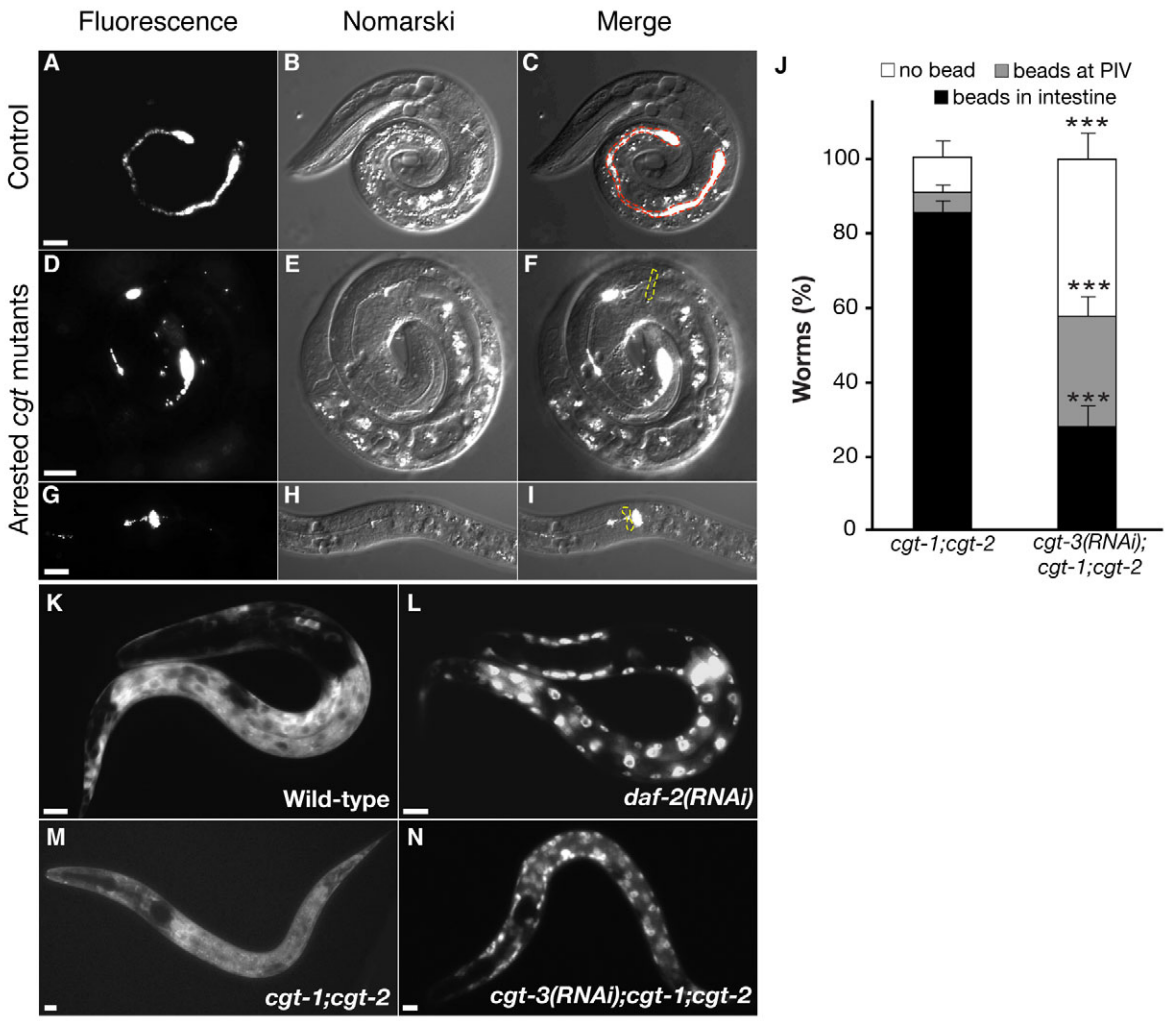

Fig. 8. CGT mutants are unable to ingest food properly and starve. *cgt-1(qa1809);cgt-2(tm1192)* L1 larvae (control, A-C) or arrested *cgt-1(qa1809);cgt-2(tm1192)* treated with *cgt-3* RNAi (D-I) animals were exposed to fluorescent beads mixed with food for 2 hours. Beads were detected in the intestinal tract (dashed red line in C) of most control animals, whereas most *cgt-3;cgt-1;cgt-2* worms had beads stuck just before (D) or just after (G) the PIV (yellow dashed line in F and I). (J) Quantification of fluorescent beads in the digestive tract. Mean ± s.e.m.; ***P<0.0001. (K-N) DAF-16::GFP localization in L1 larvae. DAF-16::GFP localizes in the cytoplasm under normal conditions and in the nucleus under starvation/stress conditions (Henderson and Johnson, 2001). In wild-type (K) and *cgt-1(qa1809);cgt-2(tm1192)* (M) L1 animals, DAF-16::GFP is detected in the cytoplasm, while it is mainly nuclear in *cgt-3(RNAi);cgt-1(qa1809);cgt-2(tm1192)* (N), and in *daf-2(RNAi)* animals (L). DAF-2 normally inhibits DAF-16 nuclear localization. Scale bars: 10 µm.

Discussion

Glycosphingolipids are thought to be essential membrane components of mammalian cells. However, the generation of mice defective in GSL production has not clarified GSL functions in vivo. By inactivating the genes required for GSL synthesis in *C. elegans*, we have generated GSL-depleted worms and show that they cannot develop beyond the first larval stage. Unexpectedly, we can rescue this growth defect by restoring CGT function in only a few cells of the digestive tract, suggesting that GSLs are dispensable in most *C. elegans* cells.

All three *C. elegans* genes encoding CGT-1, CTG-2 and CTG-3 are likely to have CGT activity. CGT-2 and CGT-3 catalyze the formation of GlcCer in cells that normally do not produce GSLs (Ichikawa and Hirabayashi, 1998; Leipelt et al., 2001), and deletion of the *cgt-1* gene reduces GlcCer levels in mutant worms (Fig. 4, compare lanes 4 and 6). It is unlikely that *C. elegans* has other genes with CGT activity, because BLAST analyses with human CGT against the entire worm genome only identify CGT-1, CGT-2 and CGT-3.

Both *cgt-1* and *cgt-3* are expressed in the PIV, IRV, RGCs, intestinal cells (particularly in the most anterior and the most posterior ones) and pharyngeal muscles. Inactivation of both these genes together causes growth arrest at the L1 stage. *cgt-1* can compensate for the lack of *cgt-3*, and vice versa, indicating that the two genes have partially overlapping functions, at least in some tissues. It is unclear why *C. elegans* has two genes that apparently catalyze the same enzymatic reaction (humans, mice and *Drosophila* have just one CGT gene) and are both expressed in some tissues. Although it is possible that they are expressed in a temporally different manner, we find that CGT-1::GFP and CGT-3::GFP are both expressed around the time when they are required: approximately at the L1 stage. Alternatively, CGT-1 and CGT-3 might catalyze glucose addition to slightly different ceramide species, with each species compensating for the absence of the other.

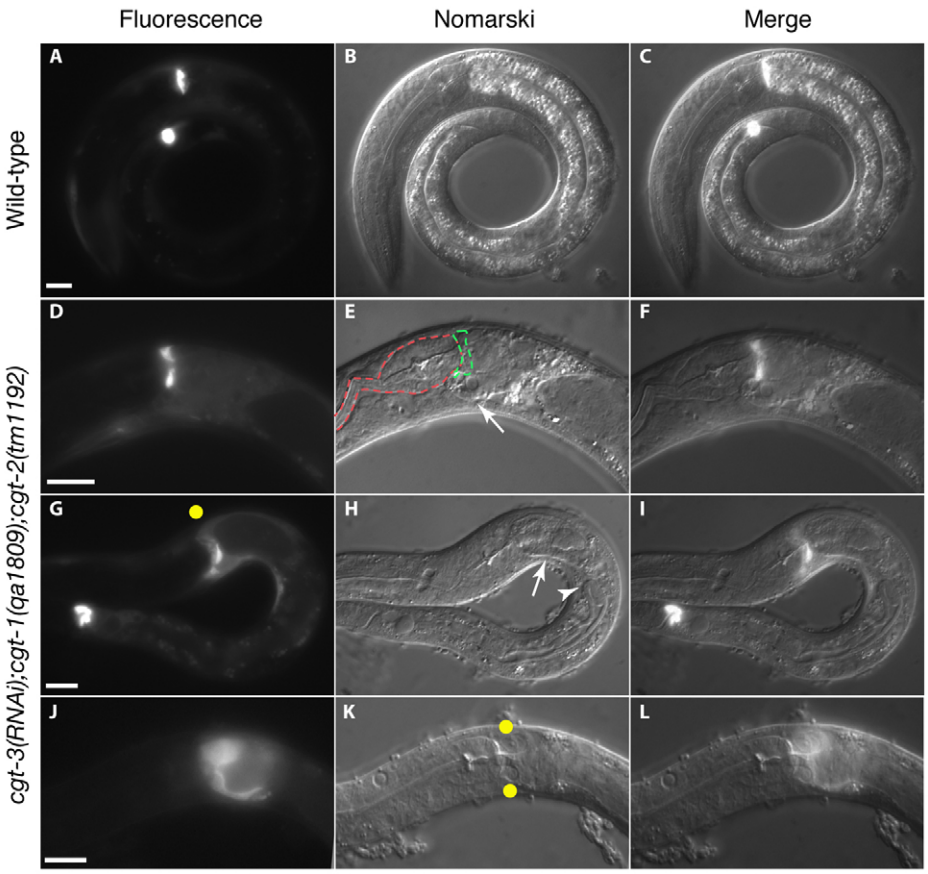

Fig. 9. CGT triple mutants show abnormal morphology of the intestinal and PIV cells. (A-C) Wild-type L1 animals expressing *F54D5.1p::gfp* in the PIV and in the IRV. The intestinal lumen appears thin and continuous. (D-L) *cgt-3;cgt-1;cgt-2* L1-arrested larvae expressing *F54D5.1p::gfp*. (D-F) CGT triple mutants arrested for 1 day showed morphologically normal PIV cells (surrounded by a green dashed line, E). However, the anterior intestinal cells appeared swollen and vacuolated (white arrow, E), and the intestinal lumen was enlarged. A red dashed line surrounds the pharynx (E). (G-L) After 3 days of L1 arrest, CGT triple mutants showed more severe defects. The PIV cells lost most of their fluorescence (spot in G), suggesting that they were dying, or became swollen (spots, K) with diffuse GFP staining (J-L). The anterior intestine appeared disorganized (arrow, H) and the intestinal tract was discontinuous in some places (arrowhead, H). Alleles: *cgt-1(qa1809)*, *cgt-2(tm1192)*, *cgt-3(RNAi)*. Scale bars: 10 μm.

Expression of *cgt-1* or *cgt-3* in PIV, IRV, and the intestinal cells adjacent to them or expression of *cgt-1* exclusively in the intestine, is sufficient to rescue the growth-arrest phenotype. The rescued animals do not show any obvious phenotype when viewed in a dissecting microscope, implying that most cells can develop and function with virtually no *cgt* activity. Such cells are likely to be essentially devoid of GSLs, because the *C. elegans* genome does not encode other CGTs, and GSLs are not likely to move from cell to cell. Our inability to rescue the CGT mutant phenotype by expressing the genes in certain tissues or by providing a mixture of exogenous GSLs (data not shown) confirms that CGTs and GSLs do not move from one cell to another.

On the one hand, CGT-knockout mice die at around E7.5, probably because many of their cells undergo apoptosis; on the other hand, cell proliferation is unaffected (Yamashita et al., 1999). It is unclear whether the increased apoptosis is caused by increased levels of ceramide, a known pro-apoptotic factor, or by GSL depletion, because it was not possible to quantify ceramide in mutant embryos. Remarkably, ES cells from CGT-knockout mice survive in vitro. These findings in mice led to the hypothesis that GSLs might be required for cell-cell or cell-matrix interactions (Yamashita et al., 1999). We find that enzymes required for GSL synthesis are only required in *C. elegans* in a subset of cells in the digestive tract and are therefore dispensable in most tissues, including the nervous system. This is surprising, because in mammals, GSLs have been implicated in a wide variety of cell functions that are expected to be essential in vivo, including intracellular protein sorting (Sprong et al., 2001), neuronal development (Futerman et al., 1999), and cell adhesion and migration (Iwabuchi et al., 1998; Hakomori and Handa, 2002). It seems that GSLs have extended their essential function from a few cell types to many cell types during evolution.

It is not clear what essential functions the GSLs serve in the intestinal cells in *C. elegans*, where normal GSL levels are required. One day after growth has arrested, intestinal cells become swollen and vacuolated, and soon after, the PIV and IRV cells also become swollen and vacuolated. These cell changes do not depend on starvation, because starved controls do not display such changes. The finding that PIV, IRV and intestinal cells appear normal at hatching in CGT mutants suggests that having essentially no GSLs is compatible with correct development of these cells. Instead, normal GSL levels appear to be essential to keep these cells alive and normal. Because we could rescue the growth-arrest phenotype by expressing CGT exclusively in the intestine or in the PIV, the IRV and in their adjacent intestinal cells, it is likely that GSLs are only essential in the most anterior and most posterior intestinal cells, which make contact with the PIV and the IRV. Our results suggest that the death or dysfunction of these cells impairs feeding, causing the worms to starve and arrest growth at the early L1 stage. Further studies will be required to understand how GSLs promote the survival and normal function of these intestinal cells and whether their survival-promoting effects are direct or indirect.

Why can cells with strongly reduced GSL levels survive in CGT mutants? It is possible that these cells adapt to the depletion of GSLs and use alternative molecules to serve the functions of the missing lipids. Such compensation happens in mammals. For example, mice that cannot synthesize galactosphingolipids, which are particularly enriched in myelin, substitute them with glucosphingolipids, which are normally absent from myelin; although this substitution allows

myelin to be made, myelin function is abnormal (Coetzee et al., 1996). It is likely that compensatory lipids are also synthesized by CGT-impoverished worms. Consistent with this possibility, we identified an enzyme involved in the modification of ceramide fatty acids in a screen for mutations synthetically lethal with *cgt-3(qa1809)* (G.M.L., unpublished results). Perhaps, because they are relatively simple organisms, worms can change their lipid composition without compromising the survival or function of most of their cells.

Materials and Methods

Nematode strains

C. elegans strains were cultured under standard conditions (Brenner, 1974). We used the following strains: LZ64, *dpy-20(e1282);cgt-1(qa1809);gxEx64[cgt-1::gfp;pMH86;pBluescript]*; LZ65, *cgt-2(tm1097)*; LZ66, *cgt-3(tm504)*; LZ68, *cgt-1(tm1027)*; LZ69, *cgt-2(tm1192)*; LZ83, *cgt-3(tm504);+/DnT1;cgt-1(tm1027)/DnT1*; LZ96, *cgt-3(tm504);dpy-20(e1282);gxEx96[cgt-3::gfp;pMH86;pBluescript]*; LZ113, *cgt-3(tm504);+/DnT1;cgt-1(qa1809)/DnT1;cgt-2(tm1097)*; LZ114, *cgt-3(tm504);+/DnT1;cgt-1(qa1809)/DnT1;cgt-2(tm1192)*; LZ163, *dpy-20(e1282);gxEx163-[F54D5.1p::gfp;pMH86;pBluescript]*; LZ196, *dpy-20(e1282);cgt-1(qa1809);cgt-2(tm1192);gxEx163*; LZ255, *cgt-3(tm504);+/DnT1;cgt-1(qa1809)/DnT1*; LZ269, *cgt-1(qa1809);zIs356[daf-16::gfp;pRF4]*; LZ278, *cgt-3(tm504);cgt-1(tm1027);cgt-2(tm1192);gxEx145[F54D5.1p::cgt-1, pPD118.33, pBluescript]*; LZ279, *cgt-3(tm504);cgt-1(qa1809);cgt-2(tm1192);gxEx145*; MT1522, *ced-3(n717)*; MT2547, *ced-4(n1162)*; MT4770, *ced-9(n1950)*; PD4667, *dpy-20(e1282);ayIs7(pBH47.70+pMH86)]*; TJ356, *zIs356[daf-16::gfp;pRF4]*; XA1809, *cgt-1(qa1809)*.

We also used various stable lines of the following transgenic strains: *dpy-20(e1282);cgt-1(qa1809);gxEx[myo-2p::cgt-1, pMH86, pBluescript]*, *dpy-20(e1282);cgt-1(qa1809);gxEx[elt-2p::cgt-1, pMH86, pBluescript]*, *cgt-3(tm504);+/DnT1;cgt-1(tm1027)/DnT1;gxEx[unc-119p::cgt-3, pPD118.33, pBluescript]*, *cgt-3(tm504);+/DnT1;cgt-1(tm1027)/DnT1;gxEx[unc-119p::cgt-1, pPD118.33, pBluescript]*, *cgt-3(tm504);+/DnT1;cgt-1(tm1027)/DnT1;gxEx[myo-3p::cgt-3, pPD118.33, pBluescript]*, *cgt-3(tm504);+/DnT1;cgt-1(tm1027)/DnT1;gxEx[F54D5.1p::cgt-1, pPD118.33, pBluescript]*, *cgt-3(tm504);+/DnT1;cgt-1(tm1027)/DnT1;gxEx[F54D5.1p::cgt-3, pPD118.33, pBluescript]*.

When not indicated otherwise, *cgt-3;cgt-1* animals were *cgt-3(tm504);cgt-1(tm1027)* from LZ83 mothers, *cgt-3(tm504);cgt-1(qa1809)* from LZ255 mothers, *cgt-3(RNAi);cgt-1(1027)*, or *cgt-3(RNAi);cgt-1(qa1809)*.

Generation of CGT gene deletions

To isolate deletions of the genes encoding CGT, we constructed a DNA library of approximately 1,400,000 haploid genomes from wild-type animals mutagenized with ethylmethane sulfonate (Lesa, 2006). Using PCR with *cgt-1* primers (Jansen et al., 1997), we isolated the deletion *cgt-1(qa1809)*. The deletion alleles *cgt-1(tm1027)*, *cgt-2(tm1097)*, *cgt-2(tm1192)* and *cgt-3(tm504)* were a generous gift from Shoehi Mitani (National Bioresource Project for the Experimental Animal 'Nematode *C. elegans*', Tokyo Women's Medical University, Tokyo, Japan) and their molecular details are available at http://www.shigen.nig.ac.jp/c.elegans/mutants/index.jsp?lang=english. *cgt-1(qa1809)* lacks the fragment comprising base pairs 20,621-21,528 of cosmid T06C12. We used PCR-based genotyping on all deleted mutants to detect the deletion and to verify that no duplications of the intact CGT genes were present (not shown). We used the following primers:: GL147, GL184, GL185 for *cgt-1(qa1809)*, GL421, GL422b, GL423b for *cgt-1(tm1027)*: GL424, GL425b, GL426b for *cgt-2(tm1097)* and *cgt-2(tm1192)*, and GL415, GL416, GL417 for *cgt-3(tm504)*. Primer sequences are available in supplementary material Table S1.

Scoring growth

Mothers of *cgt-3;cgt-1* or *cgt-3;cgt-1;cgt-2* progeny or mothers carrying one or more CGT mutations exposed to siRNA for a different CGT gene, were transferred to OP-50 plates and their progeny was observed for 5 days. Growth arrest was defined as the inability of ~100% of the progeny to pass the L2 stage by day 4-5.

Reverse transcription and sequencing of *cgt-2* alleles

Total RNA was extracted from mixed stage populations of *cgt-1(qa1809);cgt-2(tm1097)* or *cgt-1(qa1809);cgt-2(tm1192)* worms using the RNeasy kit (Qiagen, Crawley, UK). 1.5 µg total RNA per sample was reverse transcribed with Superscript II Reverse Transcriptase (Invitrogen) and hexamer random primers (Promega, Southampton, UK) to a final volume of 30 µl. 5 µl cDNA solution was PCR amplified with primers GL599 and GL600. The bands obtained were extracted with the Qiaquik Gel Extraction kit (Qiagen) and sequenced.

DNA constructs and plasmids for RNAi experiments

Full-length *cgt-1::gfp* and *cgt-3::gfp* under the control of their respective endogenous promoter were generated by fusion PCR (Hobert, 2002) using the following primers and pPD95.75 as template for *gfp::3′UTR-unc-54* sequences. For *cgt-1*: GL171, GL410, GL411 and GL412. For *cgt-3*: GL410, GL459, GL460 and GL461. *myo-2p::cgt-1* was obtained by inserting an *Nhe*I-*Sac*I fragment containing the *cgt-1* coding sequence between *myo-2* promoter and *unc-54* 3′ UTR. *elt-2p::cgt-1* was made by PCR amplifying the *elt-2* promoter with primers GL664 and GL665 and *cgt-1::unc-54 3′UTR* with primers GL666 and GL409. The two fragments were fused by PCR with primers GL667 and GL410. A similar procedure was used for *unc-119p::cgt-1* and *unc-119::cgt-3*, using primers GL545 and GL549 (to amplify the *unc-119* promoter for *cgt-1*) or GL545 and GL548 (*unc-119* promoter for *cgt-3*), GL552 and GL409 (*cgt-1* coding region) or GL551 and GL409 (*cgt-3* coding region) and GL546 andGL410 to fuse the fragments. Similarly, *myo-3p::cgt-3* was obtained with primers GL540 and GL543 (*myo-3* promoter for *cgt-3*), GL551 and GL409 (*cgt-3* coding region) and GL541 and GL410 (to fuse fragments). A similar procedure was used to obtain *F54D5.1p::cgt-1* and *F54D5.1p::cgt-3* using primers GL565 and GL569 (*F54D5.1* promoter for *cgt-1*) or GL565 and GL568 (*F54D5.1* promoter for *cgt-3*), GL551 and GL409 (*cgt-3* coding region) or GL552 and GL409 (*cgt-1* coding region) and GL566 and GL410 (to fuse fragments).

To test directly where *F54D5.1p* drives expression, we used the same strategy described above to make *F54D5.1p::gfp*. Primers GL565 and GL582 were used to amplify the *F54D5.1* promoter. *gfp* was amplified from plasmid pPD95.75 with primers GL408 and GL409. The two fragments were fused by PCR with primers GL566 and GL410. We observed GFP expression in the PIV, IRV, the RGCs, often in the most anterior and posterior intestinal cells and, rarely, in the cuticle basal membrane. Constructs were injected (Mello et al., 1991), along with the appropriate markers, in the gonad of various *cgt* mutant or N2 mothers at 0.5-50 ng/µl. Their presence was verified by PCR. Rescue was determined by the ability of the transgenic lines to grow (see above).

For double-stranded RNA generation in vitro, an 850 bp fragment of cosmid F59G1 (oligos GL134 and GL135) and an 800 bp fragment of cosmid T06C12 (oligos GL147 and GL148) were PCR amplified and cloned into pBluescript in sense (pGL179 and pGL192) and antisense (pGL180 and pGL193) orientation. Single-stranded RNA was produced in vitro from each plasmid, using T3 and T7 RiboMax kits (final volume 20 µl). Sense and antisense RNA strands were mixed, extracted with phenol-chloroform and precipitated. They were then denatured at 68°C for 10 minutes and allowed to anneal at 37°C for 30 minutes. Double-stranded RNA was resuspended in 10 µl TE, loaded into a needle and injected in the gonad.

For RNAi by feeding, a *Not*I-*Xho*I fragment from pGL179 or from pGL192 was ligated with plasmid L4440 (a gift from Andrew Fire, Stanford University, CA). L4440 carries two promoters for T7 RNA polymerase facing each other (Timmons and Fire, 1998). To visualize the M cells, the integrated *hlh-8::gfp* reporter transgene *ayIs7* from strain PD4667 was used (Harfe et al., 1998). Larvae hatch with one M cell that divides after 5-6 hours at 20°C resulting in two GFP-positive M cells. These divide again 8-9 hours after hatching (4 GFP-positive M cells), 10-11 hours after hatching (8 GFP-positive M cells) and again 13-14 hours after hatching (16 GFP-positive M cells). Then two of these 16 M cells divide again three times in L3 and L4 (Sulston and Horvitz, 1977).

RNAi and fluorescent bead feeding

Progeny of mothers exposed to siRNA for 3 days (Ahringer, 2006) was used for analysis. Red fluorescent microspheres (0.16 µm, Duke Scientific Corporation, Palo Alto, CA) were mixed with food and spread on NGM plates (Kormish and McGhee, 2005). The diameter of these beads is approximately five times smaller than that of *E. coli*, the bacteria that the worms feed on. 1-day-old L1 animals from strains LZ163 and LZ196 previously exposed or not to *cgt-3(RNAi)* were transferred on these plates and allowed to feed for 2 hours before observation.

Fluorescence microscopy

Live animals immobilized in 10 mM levamisole (Sigma, Poole, UK) or directly transferred on 5% noble agar pads on ice (*daf-16::gfp* worms) were observed on an Axioplan 2 epifluorescence microscope (Zeiss, Oberkoken, Germany) and images were captured using Openlab software (Improvision, Coventry, UK). Confocal microscopy was performed on a Leica TCS SP5 microscope (Leica Microsystems, Milton Keynes, UK) with a ×63 oil objective. Metamorph (Molecular Devices Ltd, Wokingham, UK), and ImageJ 1.40 software (National Institutes of Health, Bethesda, MD) were used for three-dimensional reconstructions and measurements.

Electron microscopy

Wild-type L1 and arrested nematodes were prepared in parallel, fixed by immersion in buffered aldehydes and stained in osmium tetroxide (Hall, 1995). Fixed specimens were washed in water, stained in 1% uranyl acetate, dehydrated through an ethanol series, washed in propylene oxide, and embedded in epoxy resin. Ribbons of ultrathin (40 nm) serial sections were collected. Images were obtained on a Tecnai G2 Spirit electron microscope (FEI UK Ltd, Cambridge, UK) using an Olympus Morada digital camera (Olympus Soft Imaging Solutions, Münster, Germany).

Analysis of glucosylceramides

Lipids were extracted from L1-arrested animals or from just starved mixed populations of worms containing mostly L1 animals and analysed by thin-layer chromatography, as previously described (Doering et al., 1999). Lipids corresponding to 100 µg worm

protein were applied in each lane and chromatograms were developed in chloroform:methanol:water 70:30:5. After development, plates were air-dried, sprayed with 8% (w/v) phosphoric acid containing 10% (w/v) copper sulphate, and charred at 180°C for 10 minutes. Relative intensities of GlcCer bands were deduced by quantifying their total number of pixels using Adobe Photoshop (Adobe Systems, Uxbridge, UK). The bands used for quantification (Fig. 4A, arrowhead) were those migrating above the major bacterial band. Lipids from *E. coli* HT115 (DE3) bacteria were included because this strain was used for RNAi by feeding. The two bands appearing in the bacteria lane are unlikely to be GSLs or ceramides because, to our knowledge, *E. coli* do not produce these lipids.

Protein alignment and statistical analysis

Proteins were aligned using ClustalX (http://www.clustal.org) and shaded with MacBoxshade (written by Kay Hoffman, Miltenyi Biotec GmbH, Bergisch Gladbach, Germany, and Michael Baron, Institute for Animal Health, Pirbright, UK). Significance was tested with Student's *t*-test or Chi-Square test, depending on the experiment, using Prism (GraphPad Software, San Diego, CA).

This work was supported by the Royal Society (G.M.L.), the Medical Research Council (E.M. and G.M.L.) and Cancer Research UK (G.M.L.). We thank Lucy Collinson for EM analysis, Shoei Mitani for the *cgt* deletions, Andy Fire for plasmids, Martin Raff for discussions, Giovanna Lalli, Stephen Nurrish and Martin Raff for critically reading the manuscript and Giampietro Schiavo for support during the initial stages of this work. Some nematode strains were provided by the *Caenorhabditis* Genetics Center, which is funded by the NIH National Center for Research Resources (NCRR). Deposited in PMC for release after 6 months.

References

Ahringer, J. (2006). Reverse genetics. In *Wormbook* (ed. The *C. elegans* Research Community). Wormbook, doi:10.1895/wormbook.1.47.1.

Brenner, S. (1974). The genetics of *Caenorhabditis elegans*. *Genetics* **77**, 71-94.

Byerly, L., Cassada, R. C. and Russell, R. L. (1976). The life cycle of the nematode *Caenorhabditis elegans*. I. Wild type growth and reproduction. *Dev. Biol.* **51**, 23-33.

Chen, Y. W., Pedersen, J. W., Wandall, H. H., Levery, S. B., Pizette, S., Clausen, H. and Cohen, S. M. (2007). Glycosphingolipids with extended sugar chain have specialized functions in development and behavior of *Drosophila*. *Dev. Biol.* **306**, 736-749.

Chitwood, D. J., Lusby, W. R., Thompson, M. J., Kochansky, J. P. and Howarth, O. W. (1995). The glycosylceramides of the nematode *Caenorhabditis elegans* contain an unusual, branched-chain sphingoid base. *Lipids* **30**, 567-573.

Coetzee, T., Fujita, N., Dupree, J., Shi, R., Blight, A., Suzuki, K. and Popko, B. (1996). Myelination in the absence of galactocerebroside and sulfatide: normal structure with abnormal function and regional instability. *Cell* **86**, 209-219.

Degroote, S., Wolthoorn, J. and van Meer, G. (2004). The cell biology of glycosphingolipids. *Semin. Cell Dev. Biol.* **15**, 375-387.

Deng, W., Li, R. and Ladisch, S. (2000). Influence of cellular ganglioside depletion on tumor formation. *J. Natl. Cancer Inst.* **92**, 912-917.

Doering, T., Holleran, W. M., Potratz, A., Vielhaber, G., Elias, P. M., Suzuki, K. and Sandhoff, K. (1999). Sphingolipid activator proteins are required for epidermal permeability barrier formation. *J. Biol. Chem.* **274**, 11038-11045.

Entchev, E. V., Schwudke, D., Zagoriy, V., Matyash, V., Bogdanova, A., Habermann, B., Zhu, L., Shevchenko, A. and Kurzchalia, T. V. (2008). LET-767 is required for the production of branched chain and long chain fatty acids in *Caenorhabditis elegans*. *J. Biol. Chem.* **283**, 17550-17560.

Fukushige, T., Hawkins, M. G. and McGhee, J. D. (1998). The GATA-factor *elt-2* is essential for formation of the *Caenorhabditis elegans* intestine. *Dev. Biol.* **198**, 286-302.

Furukawa, K., Tokuda, N., Okuda, T. and Tajima, O. (2004). Glycosphingolipids in engineered mice: insights into function. *Semin. Cell Dev. Biol.* **15**, 389-396.

Futerman, A. H., Boldin, S. A., Brann, A. B., Pelled, D., Meivar-Levy, I. and Zisling, R. (1999). Regulation of sphingolipid and glycosphingolipid metabolism during neuronal growth and development. *Biochem. Soc. Trans.* **27**, 432-437.

Goode, S., Wright, D. and Mahowald, A. P. (1992). The neurogenic locus brainiac cooperates with the Drosophila EGF receptor to establish the ovarian follicle and to determine its dorsal-ventral polarity. *Development* **116**, 177-192.

Goode, S., Melnick, M., Chou, T. B. and Perrimon, N. (1996). The neurogenic genes *egghead* and *brainiac* define a novel signaling pathway essential for epithelial morphogenesis during *Drosophila* oogenesis. *Development* **122**, 3863-3879.

Griffitts, J. S., Huffman, D. L., Whitacre, J. L., Barrows, B. D., Marroquin, L. D., Muller, R., Brown, J. R., Hennet, T., Esko, J. D. and Aroian, R. V. (2003). Resistance to a bacterial toxin is mediated by removal of a conserved glycosylation pathway required for toxin-host interactions. *J. Biol. Chem.* **278**, 45594-45602.

Griffitts, J. S., Haslam, S. M., Yang, T., Garczynski, S. F., Mulloy, B., Morris, H., Cremer, P. S., Dell, A., Adang, M. J. and Aroian, R. V. (2005). Glycolipids as receptors for Bacillus thuringiensis crystal toxin. *Science* **307**, 922-925.

Groux-Degroote, S., van Dijk, S. M., Wolthoorn, J., Neumann, S., Theos, A. C., De Maziere, A. M., Klumperman, J., van Meer, G. and Sprong, H. (2008). Glycolipid-dependent sorting of melanosomal from lysosomal membrane proteins by lumenal determinants. *Traffic* **9**, 951-963.

Hakomori, S. and Handa, K. (2002). Glycosphingolipid-dependent cross-talk between glycosynapses interfacing tumor cells with their host cells: essential basis to define tumor malignancy. *FEBS Lett.* **531**, 88-92.

Hall, D. H. (1995). Electron microscopy and three-dimensional image reconstruction. *Methods Cell Biol.* **48**, 395-436.

Hall, D. H. and Altun, Z. F. (2008). *C. elegans Atlas*. Cold Spring Harbor, NY: Cold Spring Harbor Laboratory Press.

Haltiwanger, R. S. and Lowe, J. B. (2004). Role of glycosylation in development. *Annu. Rev. Biochem.* **73**, 491-537.

Harfe, B. D., Branda, C. S., Krause, M., Stern, M. J. and Fire, A. (1998). MyoD and the specification of muscle and non-muscle fates during postembryonic development of the *C. elegans* mesoderm. *Development* **125**, 2479-2488.

Henderson, S. T. and Johnson, T. E. (2001). *daf-16* integrates developmental and environmental inputs to mediate aging in the nematode *Caenorhabditis elegans*. *Curr. Biol.* **11**, 1975-1980.

Hengartner, M. O. and Horvitz, H. R. (1994). Programmed cell death in *Caenorhabditis elegans*. *Curr. Opin. Genet. Dev.* **4**, 581-586.

Hobert, O. (2002). PCR fusion-based approach to create reporter gene constructs for expression analysis in transgenic *C. elegans*. *Biotechniques* **32**, 728-730.

Hong, Y., Roy, R. and Ambros, V. (1998). Developmental regulation of a cyclin-dependent kinase inhibitor controls postembryonic cell cycle progression in *Caenorhabditis elegans*. *Development* **125**, 3585-3597.

Hope, I. A., Stevens, J., Garner, A., Hayes, J., Cheo, D. L., Brasch, M. A. and Vidal, M. (2004). Feasibility of genome-scale construction of promoter: reporter gene fusions for expression in *Caenorhabditis elegans* using a multisite gateway recombination system. *Genome Res.* **14**, 2070-2075.

Ichikawa, S. and Hirabayashi, Y. (1998). Glucosylceramide synthase and glycosphingolipid synthesis. *Trends Cell Biol.* **8**, 198-202.

Ichikawa, S., Nakajo, N., Sakiyama, H. and Hirabayashi, Y. (1994). A mouse B16 melanoma mutant deficient in glycolipids. *Proc. Natl. Acad. Sci. USA* **91**, 2703-2707.

Ichikawa, S., Sakiyama, H., Suzuki, G., Hidari, K. I. and Hirabayashi, Y. (1996). Expression cloning of a cDNA for human ceramide glucosyltransferase that catalyzes the first glycosylation step of glycosphingolipid synthesis. *Proc. Natl. Acad. Sci. USA* **93**, 4638-4643.

Iwabuchi, K., Yamamura, S., Prinetti, A., Handa, K. and Hakomori, S. (1998). GM3-enriched microdomain involved in cell adhesion and signal transduction through carbohydrate-carbohydrate interaction in mouse melanoma B16 cells. *J. Biol. Chem.* **273**, 9130-9138.

Jansen, G., Hazendonk, E., Thijssen, K. L. and Plasterk, R. H. (1997). Reverse genetics by chemical mutagenesis in *Caenorhabditis elegans*. *Nat. Genet.* **17**, 119-121.

Jennemann, R., Sandhoff, R., Wang, S., Kiss, E., Gretz, N., Zuliani, C., Martin-Villalba, A., Jager, R., Schorle, H., Kenzelmann, M. et al. (2005). Cell-specific deletion of glucosylceramide synthase in brain leads to severe neural defects after birth. *Proc. Natl. Acad. Sci. USA* **102**, 12459-12464.

Johnson, T. E., Mitchell, D. H., Kline, S., Kemal, R. and Foy, J. (1984). Arresting development arrests aging in the nematode *Caenorhabditis elegans*. *Mech. Ageing Dev.* **28**, 23-40.

Katic, I., Vallier, L. G. and Greenwald, I. (2005). New positive regulators of lin-12 activity in Caenorhabditis elegans include the BRE-5/Brainiac glycosphingolipid biosynthesis enzyme. *Genetics* **171**, 1605-1615.

Kniazeva, M., Crawford, Q. T., Seiber, M., Wang, C. Y. and Han, M. (2004). Monomethyl branched-chain fatty acids play an essential role in *Caenorhabditis elegans* development. *PLoS Biol.* **2**, E257.

Kniazeva, M., Euler, T. and Han, M. (2008). A branched-chain fatty acid is involved in post-embryonic growth control in parallel to the insulin receptor pathway and its biosynthesis is feedback-regulated in *C. elegans*. *Genes Dev.* **22**, 2102-2110.

Kohyama-Koganeya, A., Sasamura, T., Oshima, E., Suzuki, E., Nishihara, S., Ueda, R. and Hirabayashi, Y. (2004). *Drosophila* glucosylceramide synthase: a negative regulator of cell death mediated by proapoptotic factors. *J. Biol. Chem.* **279**, 35995-36002.

Kolesnick, R. N. and Kronke, M. (1998). Regulation of ceramide production and apoptosis. *Annu. Rev. Physiol.* **60**, 643-665.

Kormish, J. D. and McGhee, J. D. (2005). The *C. elegans* lethal gut-obstructed *gob-1* gene is trehalose-6-phosphate phosphatase. *Dev. Biol.* **287**, 35-47.

Lahiri, S. and Futerman, A. H. (2007). The metabolism and function of sphingolipids and glycosphingolipids. *Cell. Mol. Life Sci.* **64**, 2270-2284.

Leipelt, M., Warnecke, D., Zahringer, U., Ott, C., Muller, F., Hube, B. and Heinz, E. (2001). Glucosylceramide synthases, a gene family responsible for the biosynthesis of glucosphingolipids in animals, plants, and fungi. *J. Biol. Chem.* **276**, 33621-33629.

Lesa, G. M. (2006). Isolation of *Caenorhabditis elegans* gene knockouts by PCR screening of chemically mutagenized libraries. *Nat. Protocols* **1**, 2231-2240.

Li, R., Manela, J., Kong, Y. and Ladisch, S. (2000). Cellular gangliosides promote growth factor-induced proliferation of fibroblasts. *J. Biol. Chem.* **275**, 34213-34223.

Maine, E. M. (2001). RNAi As a tool for understanding germline development in *Caenorhabditis elegans*: uses and cautions. *Dev. Biol.* **239**, 177-189.

Marks, D. L., Wu, K., Paul, P., Kamisaka, Y., Watanabe, R. and Pagano, R. E. (1999). Oligomerization and topology of the Golgi membrane protein glucosylceramide synthase. *J. Biol. Chem.* **274**, 451-456.

Marks, D. L., Dominguez, M., Wu, K. and Pagano, R. E. (2001). Identification of active site residues in glucosylceramide synthase. A NUCLEOTIDE-BINDING/CATALYTIC MOTIF CONSERVED WITH PROCESSIVE beta-GLYCOSYLTRANSFERASES. *J. Biol. Chem.* **276**, 26492-26498.

Mello, C. C., Kramer, J. M., Stinchcomb, D. and Ambros, V. (1991). Efficient gene transfer in *C. elegans* after microinjection of DNA into germline cytoplasm: extrachromosomal maintenance and integration of transforming sequences. *EMBO J.* **10**, 3959-3970.

Munro, S. (2003). Lipid rafts: elusive or illusive? *Cell* **115**, 377-388.

Okkema, P. G., Harrison, S. W., Plunger, V., Aryana, A. and Fire, A. (1993). Sequence requirements for myosin gene expression and regulation in *Caenorhabditis elegans*. *Genetics* **135**, 385-404.

Pettus, B. J., Chalfant, C. E. and Hannun, Y. A. (2002). Ceramide in apoptosis: an overview and current perspectives. *Biochim. Biophys. Acta* **1585**, 114-125.

Simons, K. and Ikonen, E. (1997). Functional rafts in cell membranes. *Nature* **387**, 569-572.

Sprong, H., Degroote, S., Claessens, T., van Drunen, J., Oorschot, V., Westerink, B. H., Hirabayashi, Y., Klumperman, J., van Der Sluijs, P. and van Meer, G. (2001). Glycosphingolipids are required for sorting melanosomal proteins in the Golgi complex. *J. Cell Biol.* **155**, 369-380.

Sulston, J. and Horvitz, H. R. (1977). Postembryonic cell lineages of the nematode *Caenorhabditis elegans*. *Dev. Biol.* **56**, 110-156.

Timmons, L. and Fire, A. (1998). Specific interference by ingested dsRNA. *Nature* **395**, 854.

Varki, A., Cummings, R., Esko, J. D., Freeze, H., Hart, G. and Marth, J. (1999). *Essentials of Glycobiology*. Cold Spring Harbor, NY: Cold Spring Harbor Laboratory Press.

Wu, K., Marks, D. L., Watanabe, R., Paul, P., Rajan, N. and Pagano, R. E. (1999). Histidine-193 of rat glucosylceramide synthase resides in a UDP-glucose- and inhibitor (D-threo-1-phenyl-2-decanoylamino-3-morpholinopropan-1-ol)-binding region: a biochemical and mutational study. *Biochem. J.* **341**, 395-400.

Yamashita, T., Wada, R., Sasaki, T., Deng, C., Bierfreund, U., Sandhoff, K. and Proia, R. L. (1999). A vital role for glycosphingolipid synthesis during development and differentiation. *Proc. Natl. Acad. Sci. USA* **96**, 9142-9147.

Zhang, J., Alter, N., Reed, J. C., Borner, C., Obeid, L. M. and Hannun, Y. A. (1996). Bcl-2 interrupts the ceramide-mediated pathway of cell death. *Proc. Natl. Acad. Sci. USA* **93**, 5325-5328.

Journal of Cell Science

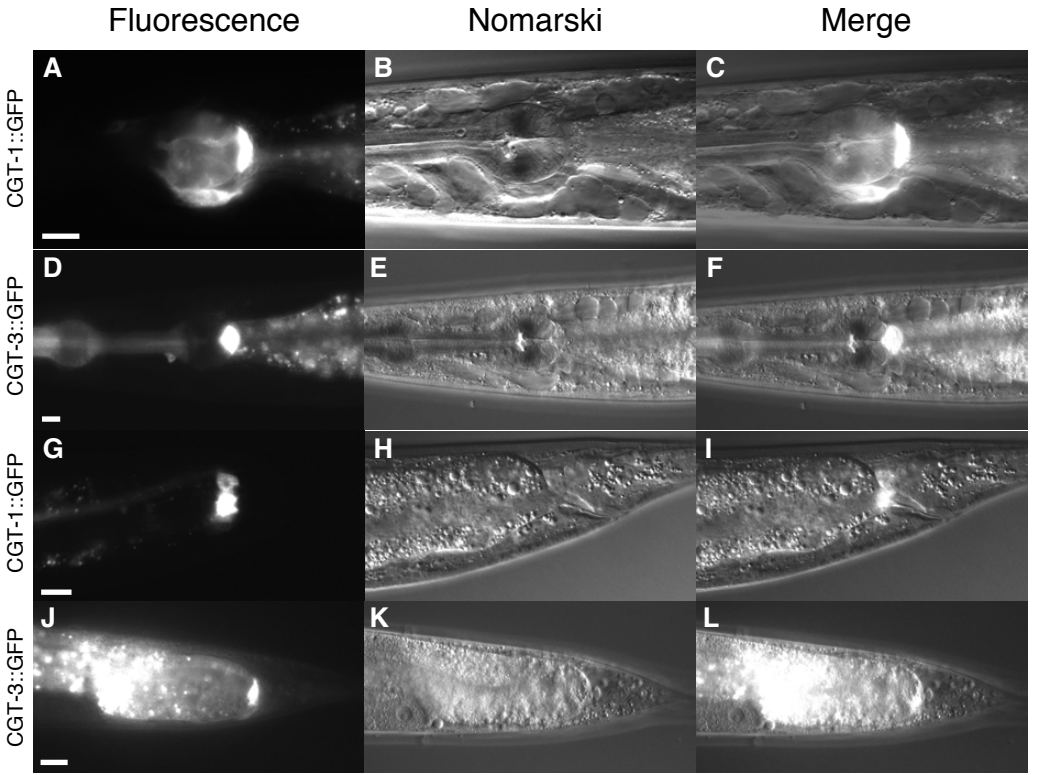
Fluorescence
Nomarski
Merge
CGT-1::GFP
CGT-3::GFP
CGT-1::GFP
CGT-3::GFP
A
B
C
D
E
F
G
H
I
J
K
L

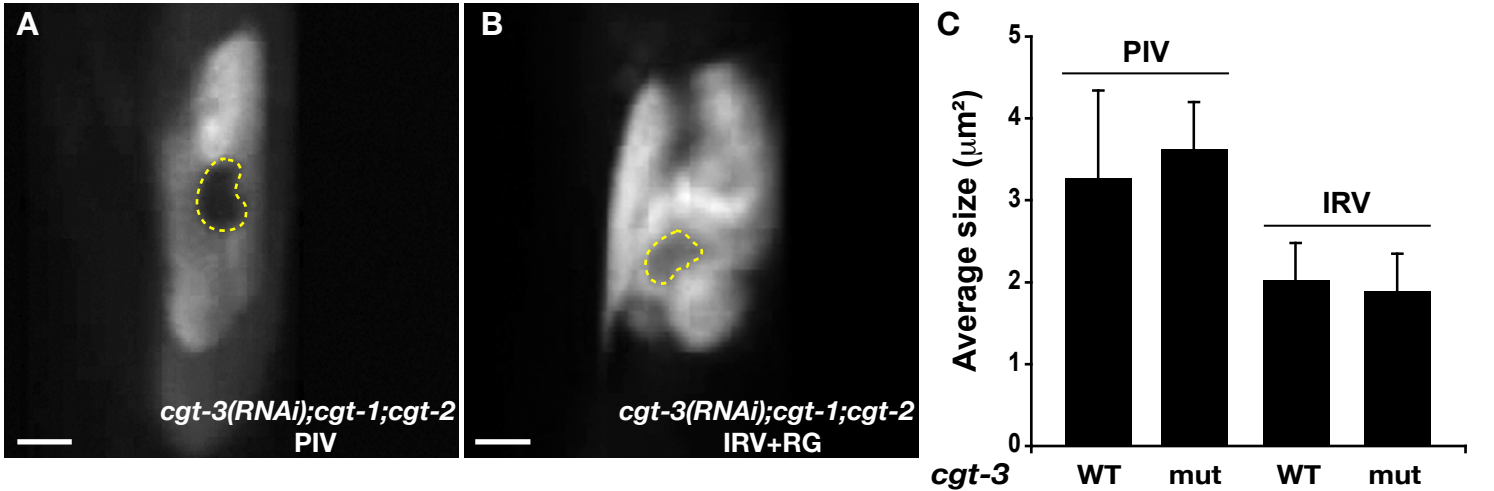
A
cgt-3(RNAi);cgt-1;cgt-2
PIV
B
cgt-3(RNAi);cgt-1;cgt-2
IRV+RG
C
Average size (μm²)
5
4
3
2
1
0
PIV
IRV
cgt-3
WT
mut
WT
mut

Table S1. PCR primers

Name	Sequence (5'->3')
GL134	CGGAATTCCTAACAATGTAACTGATGGAGAGACAACAACCC
GL135	GGGGTACCGTATTTTGGAACTTCTCATGGACG
GL147	CAGCTACCACTCCTTCATCACTAGATGCAG
GL148	CCTGTTCAAACGCTGCATGAAACCCTTGCCG
GL171	CCCGTTATATCTTCAAGCTTCGGGGTGCTC
GL184	CTAGAACAAATTGGGGAAGCG
GL185	GACTTTGAGCGACGCAGCAG
GL408	AGCTTGCATGCCTGCAGGTCGACT
GL409	AAGGGCCCGTACGGCCGACTAGTAGG
GL410	GGAAACAGTTATGTTTGGTATATTGGG
GL411	AGTCGACCTGCAGGCATGCAAGCTAACAACGGCTCCTTTCGATAATG
GL412	GTCATATTGTGACTCGTAGTTTGCCTGCC
GL415	CCAAAATTTCAGCCGTGGCGTC
GL416	CCACAGCTTCATCATCTGAAG
GL417	GAAACAATCAACATTTTGGTGG
GL421	CCCCCGGACGTCGCTAATTGG
GL422b	CACAAGTCAATACCATTCTTTCGAGC
GL423b	GCATTGTGATAACTGAGCTACCAAC
GL424	CTGCCCAACCGGAATGTCATCG
GL425b	GCGCGATCGGACAGATGCCTC
GL426b	CGTGAAGCATGATTGTTGTAAGCATATC
GL459	CTTGGGTTCTCATCACCACTTTGTGC
GL460	AGTCGACCTGCAGGCATGCAAGCTACATTTTGGTGGAAGTATCTGTCC
GL461	GTGCACTTATGTTGAATGATTACCCTTCC
GL540	AAGCTTGGGCTGCAGGTCGGCTATA
GL541	CGGCTATAATAAGTTCTTGAATAAAA
GL543	GGCCACGGCTTTTGCAACTTCCATTTCTAGATGGATCTAGTGGTCGTGGG
GL545	GATTACGCCAAGCTTCAGTAAAAG
GL546	CAGTAAAAGAAGTAGAATTTTATAG
GL548	GGCCACGGCTTTTGCAACTTCCATATATGGTACCCTCCAAGGGTCCTCCTG
GL549	TACCACTTCGTTGGCAGCCTCCATATATGGTACCCTCCAAGGGTCCTCCTG
GL551	ATGGAAGTTGCAAAAGCCGTGGCCAC
GL552	ATGGAGGCTGCCAACGAAGTGGTAAAC
GL565	CAAACCTCCGGTATCCAATTTCGC
GL566	GGCGCTGCAGTGAGGTCGACATCTC
GL568	GGCCACGGCTTTTGCAACTTCCATTTTGAAGTGTCTGCAATTATATTTTTG
GL569	TACCACTTCGTTGGCAGCCTCCATTTTGAAGTGTCTGCAATTATATTTTTG
GL582	AGTCGACCTGCAGGCATGCAAGCTCATTTTGAAGTGTCTGCAATTATATTTTTG
GL599	GGAGGTTGAGATTATTCCGG
GL600	GATCGATGGATCAAGTGCGG
GL664	GCTTGCATGCCTGCAGGTCGACTCTAGAGGATCC
GL665	CCTTTGGGTCCTTTGGCCAATCCCGGGGATCC
GL666	GGATCCCCGGGATTGGCCAAAGGACCCAAAGG
GL667	CTCTAGAGGATCCACATATTTTTTCCCGCC